REGULAR AND CHAOTIC MOTION IN GLOBULAR CLUSTERS

DANIEL D. CARPINTERO, JUAN C. MUZZIO and FELIPE C. WACHLIN

Facultad de Ciencias Astronómicas y Geofísicas - UNLP and PROFOEG – CONICET
E-mail: ddc@fcaglp.unlp.edu.ar, jcmuzzio@fcaglp.unlp.edu.ar, fcw@fcaglp.unlp.edu.ar

Abstract. As a first step towards a comprehensive investigation of stellar motions within globular clusters, we present here the results of a study of stellar orbits in a mildly triaxial globular cluster that follows a circular orbit inside a galaxy. The stellar orbits were classified using the frequency analysis code of Carpintero and Aguilar and, as a check, the Liapunov characteristic exponents were also computed in some cases.

The orbit families were obtained using different start spaces. Chaotic orbits turn out to be very common and while, as could be expected, they are particularly abundant in the outer parts of the cluster, they are still significant in the innermost regions. Their relevance for the structure of the cluster is discussed.

Key words: globular clusters – orbit classification – chaotic motion

1. Introduction

We tend to think of globular clusters as spherical stationary stellar systems that are well described by King's or Michie's models (see, e.g., (Binney and Tremaine, 1987)). Obviously, nobody in his right mind would search for chaotic motions in such systems, but the truth is that: a) Globular clusters are not spherical and exhibit different degrees of ellipticity (see, e.g., (Han and Ryden, 1994)); b) Globular clusters are not isolated systems and the motions of their stars are governed, not only by the cluster's field, but by the tidal forces of the galaxy where the cluster belongs as well. Thus, as neither angular momentum nor energy has to be conserved, it is very reasonable to expect to find chaotic motions in the stellar orbits within globular clusters.

The presence of significant chaotic motions would certainly have important consequences for the structure of the cluster and the models should take into account this fact. The present work is just a first step to show that, even under very simple hypotheses, chaotic orbits turn out to be very abundant in globular clusters, thus paving the way for future, more detailed, studies on this subject.

2. The Model

We wanted to begin our investigation of chaos in globular clusters with the simplest possible case, so that:

a) We adopted a circular orbit for the motion of the globular cluster around the galaxy.
b) We assumed that the cluster is deformed by the effect of the tidal forces only.
c) We neglected the effects of stellar encounters within the cluster.

The adoption of more realistic conditions should increase chaos because: a) With elongated cluster orbits we lose Jacobi's integral; b) More triaxial potentials might enhance chaoticity; c) Impulsive forces will contribute to chaos.

The galaxy was represented by a spherically symmetrical logarithmic potential and the globular cluster with a modified Satoh (Satoh, 1980) distribution, whose potential is:

$$\Phi_S(x,y,z) = -\frac{GM}{\sqrt{x^2 + y^2 + z^2 + g(g + 2\sqrt{y^2 + (z/b)^2 + h^2})}}. \tag{1}$$

Here the origin of coordinates lies at the center of the globular cluster, the x axis points in the direction opposite to the galactic center, the y axis in the direction of motion of the cluster around the galaxy and the z axis perpendicular to the orbital plane. Notice that we have interchanged $x^2 + y^2$ with z^2, in order to obtain a prolate (rather than Satoh's oblate) system, and that we have also divided z by a parameter b, in order to get a triaxial system (tidal deformation yields the shortest axis perpendicular to the orbital plane).

The main advantage of this election is that isodensity surfaces increase their ellipticity as we move outwards, just as it should happen with a system that is tidally deformed, as shown by the full lines in Figure 1. We have also included in the figure (dashed lines) the effective equipotential curves (i.e., those that result from adding the centrifugal term and the galactic potential to the modified Satoh potential).

The equations of motion are:

$$\ddot{x} = -\frac{GMx}{S^3} - \omega^2 R^2 \frac{R+x}{(R+x)^2 + y^2 + z^2} + \omega^2(R+x) + 2\omega\dot{y}; \tag{2}$$

$$\ddot{y} = -\frac{GMy(1+g/T)}{S^3} - \omega^2 R^2 \frac{y}{(R+x)^2 + y^2 + z^2} + \omega^2 y - 2\omega\dot{x}; \tag{3}$$

$$\ddot{z} = -\frac{GMz(1+g/(b^2 T))}{S^3} - \omega^2 R^2 \frac{z}{(R+x)^2 + y^2 + z^2}, \tag{4}$$

where

$$S = \sqrt{x^2 + y^2 + z^2 + g(g + 2T)}, \quad T = \sqrt{y^2 + (z/b)^2 + h^2}, \tag{5}$$

and M is the mass of the globular cluster, R is the radius of its orbit, and ω is its angular velocity. The Jacobi integral is:

$$E_J = \frac{1}{2}(\dot{x}^2 + \dot{y}^2 + \dot{z}^2) - \frac{1}{2}\omega^2\left[(R+x)^2 + y^2\right] + \Phi(x,y,z), \tag{6}$$

where Φ is the sum of the potential of the globular cluster, Φ_S, and that of the galaxy:

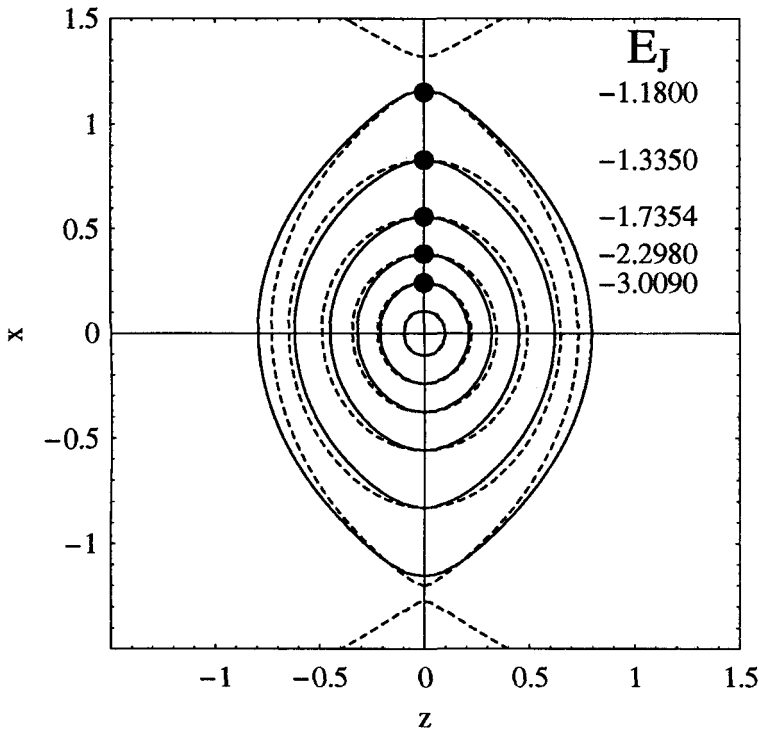$$\Phi_G(x,y,z) = \frac{1}{2}\omega^2 R^2 \ln\left[(R+x)^2 + y^2 + z^2\right]. \tag{7}$$

Fig. 1. Isodensity curves for the modified Satoh potential (full lines) in the x–z plane. The equipotentials that result from adding the centrifugal term and the galactic potential are shown as dashed lines.

We adopted the following values: $b = 0.8$, $h = 0.5$, $g = 0.05$, $R = 100$, $\omega = 0.5$, which result in a tidal radius $r_t = x_t = 1.24$, and the half–mass radius is $r_h = 0.28$.

If, for example, we choose $R = 10$ kpc and the mass of the galaxy within that radius as $M_g = 1.25 \times 10^{11} M_\odot$, then we have a tidal radius of about $r_t = 120$ pc and a cluster mass of $M = 5 \times 10^5 M_\odot$, that is, reasonable values for a globular cluster.

3. Orbital Analysis

3.1. LIAPUNOV CHARACTERISTIC EXPONENTS

D. Pfenniger kindly let us use his LIAMAG routine that computes the six Liapunov exponents following Benettin's method.

We are not so much interested on whether a specific stellar orbit is chaotic or not, as in having statistical information on a large number of orbits. Therefore,

we followed an approach similar to that of Merritt and Fridman (1996): 1) We integrated the orbits for about 10,000 orbital periods (rather than 100, as they did); 2) We used as estimator the sum of the three non–negative Liapunov exponents (also called Kolmogorov entropy); 3) We dubbed, rather arbitrarily, chaotic those orbits where:

$$\ln(s_1 + s_2 + s_3) > -5, \tag{8}$$

where the $s_i (i = 1, 2, 3)$ are the positive estimates of the Liapunov exponents after 10,000 orbital periods.

We used this method just as a check, because: 1) It only allows one to decide between regular and chaotic orbits, providing no further information on the kind of orbit one has; 2) It is very slow (about one day of computing on a Pentium Pro, 200 MHz, personal computer for 150 orbits).

3.2. FREQUENCY ANALYSIS

This technique was introduced by Binney and Spergel (1982), (1984) and extended, in a different form, by Laskar (1993). Carpintero and Aguilar (1998) refined the original method and prepared a FORTRAN code that allows one to automatically classify large numbers of orbits.

The basis of the method is that regular orbits move on a torus–like manifold and are quasi–periodic. Fourier spectra of the time series of the coordinates of a regular orbit consist of discrete lines whose frequencies are integer linear combinations of the frequencies of the angle variables. Thus, from the Fourier spectra one can classify the regular orbits. Besides, chaotic orbits yield continuous spectra and can be recognized too (see (Carpintero and Aguilar, 1998), for examples of different orbits). The main limitation of the method is the difficulty to recognize whether finite precision numbers have a rational quotient.

3.3. INITIAL CONDITIONS

We prepared sets of initial conditions for several values of the Jacobi integral $(-3.0090, -1.7354, -1.3350$ and $-1.1800)$. For each value of the integral, we selected four sets: 1) Zero initial velocity; 2) x–y plane and $\dot{z}$ initial velocity; 3) x–z plane and $\dot{y}$ initial velocity; 4) y–z plane and $\dot{x}$ initial velocity.

Schwarzschild (1993) proposed the use of the initial conditions 1 and 3 for non–rotating potentials. As we have a rotating potential, we preferred to add also initial conditions 2 and 4. We expect to have sampled the whole phase space with these sets, at the price of some possible overlap, as we will see later on.
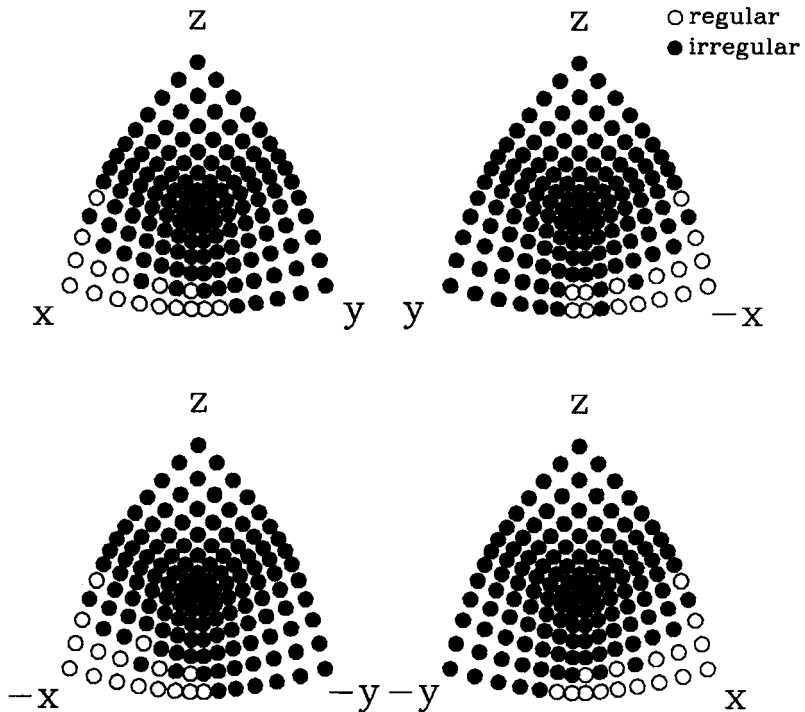
Fig. 2. Zero velocity start space for $E_J = -1.335$. The regular or irregular character of the stellar orbits was decided from the Liapunov exponents analysis.

4. Results

For every set of initial conditions we prepared colour plots showing, with different colours, the different types of stellar orbits that result from those initial conditions. Black and white examples are given in Figures 2 through 5, which correspond to a value of the Jacobi integral of $E_J = -1.335$. Figures 2 and 3 are results obtained from the Liapunov exponents analysis: Figure 2 corresponds to zero velocity initial conditions and Figure 3 to initial conditions in the x–z plane. Figures 4 and 5 are results from the frequency analysis and correspond, respectively, to the same initial conditions of Figures 2 and 3. Notice that the density of points is two orders of magnitude larger for Figures 4 and 5, resulting in much better definition, thanks to the short computing times needed for the frequency analysis. There is a generally good agreement between the results of both methods, but there are a couple of
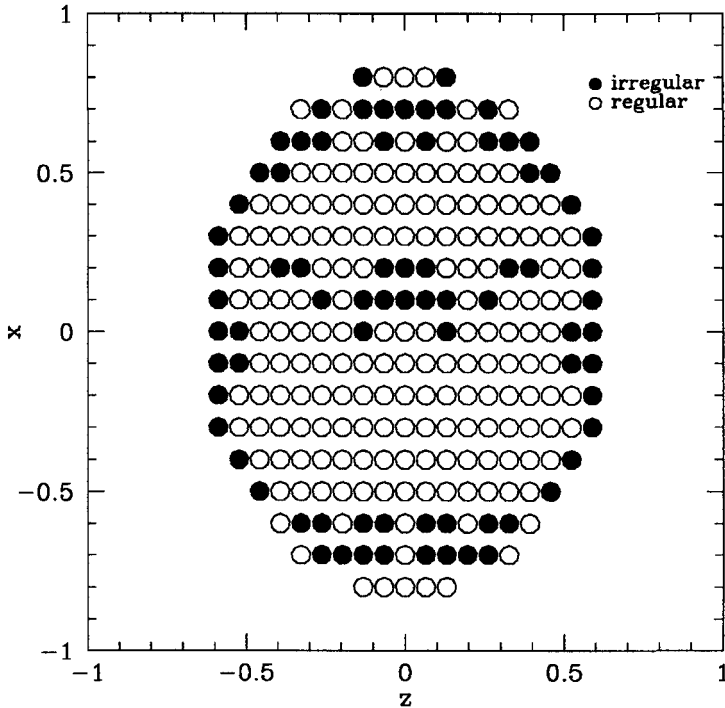
Fig. 3. $x–z$ start space for $E_J = -1.335$. The regular or irregular character of the stellar orbits was decided from the Liapunov exponents analysis.

caveats. First, a small fraction of the orbits (less than 10%) could not be classified with the frequency analysis code; from our experience with that code, we know that most of those orbits turn out to be chaotic on a more detailed analysis, so that we counted them as such. Second, the Liapunov exponents tend to give somewhat larger fractions (by about 10%) of chaotic orbits. The most likely explanation for this discrepancy comes from the very different integration times: between 100 and 200 periods for the frequency analysis and 10,000 periods for the Liapunov one; as a result, orbits that behave regularly most of the time, although they are truly chaotic, have a much larger chance of getting detected in the second case.

We noticed that the $x–z$ and $y–z$ initial conditions gave the same fractions for the different kinds of orbits, so that we suspect that with those sets of initial conditions we are sampling esentially the same parameter space. Therefore, we combined the results of both start spaces together in what follows.

Figures 6a, b and c give the fractions of the different kinds of stellar orbits, as a function of the Jacobi integral, for the zero initial velocity, $x–y$ and $x–z$ plus $y–z$ start spaces, respectively. Boxes and chaotic orbits clearly dominate for zero initial velocity conditions, while small–axis tubes are the most abundant orbits in
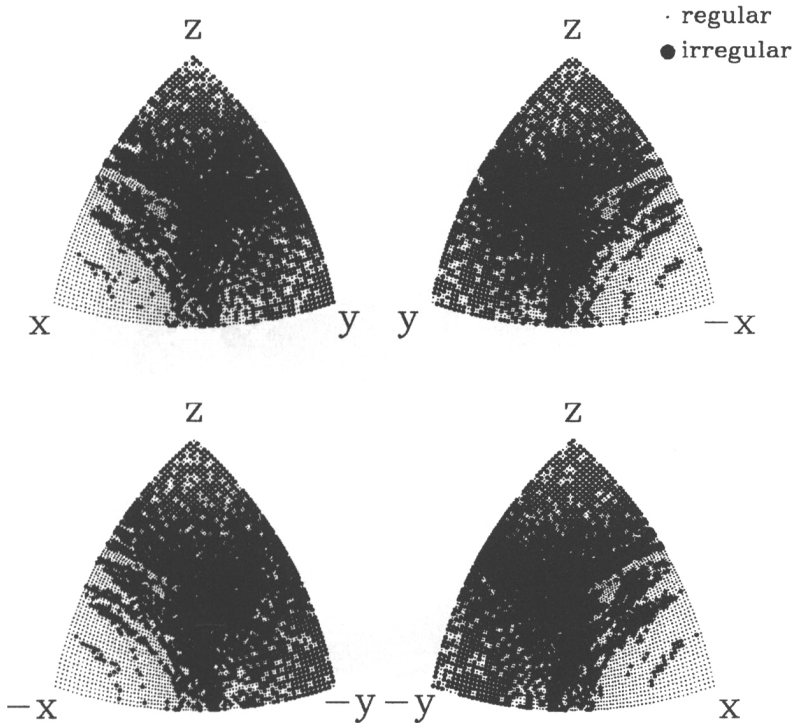
Fig. 4. Zero velocity start space for $E_J = -1.335$. The regular or irregular character of the stellar orbits was decided from the frequency analysis. The bulk of the regular orbits are long–axis boxes, as shown by their proximity to the x–axis.

the other cases. Long–axis tubes are almost non–existent. As expected, chaotic orbits predominate for low absolute values of the Jacobi integral, i.e., mainly in the outermost parts of the globular cluster. Nevertheless, chaos is still significant for $E_J = -3.009$, with 37% of the orbits with zero initial velocity, 35% of those on the x–y start space and 21% of those on the x–z and y–z start spaces. These results are particularly important because the zero velocity $E_J = -3.009$ surface encloses about 50% of the total mass of the globular cluster, so that chaos is present well inside the cluster and, moreover, seems to dominate in its outer half.
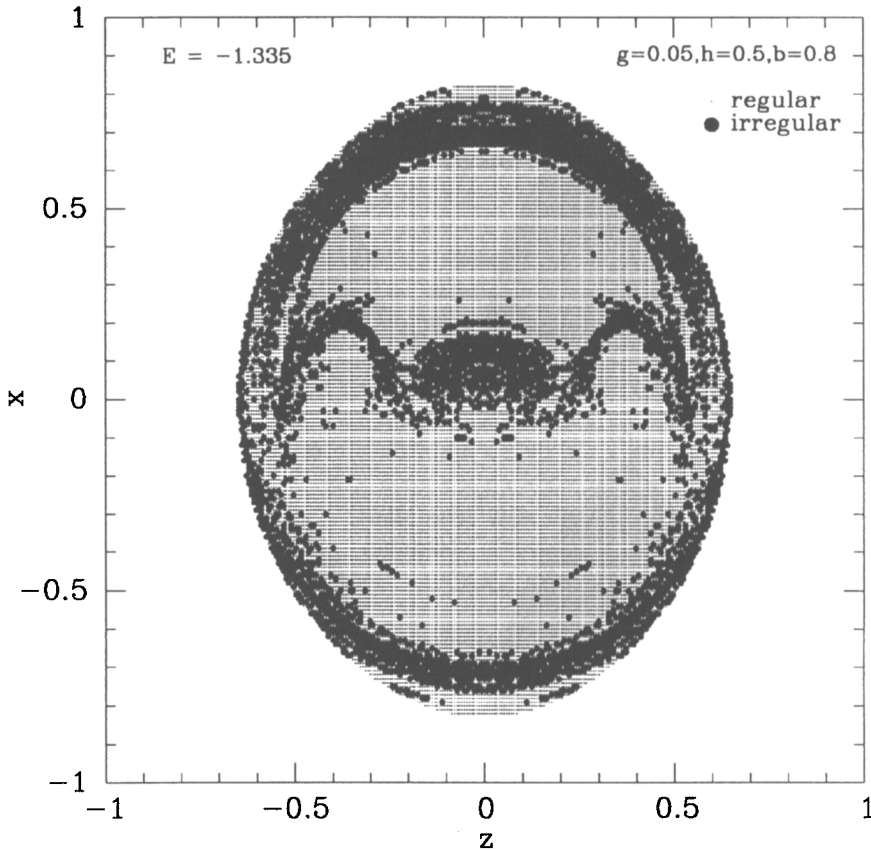
Fig. 5. x–z start space for $E_J = -1.335$. The regular or irregular character of the stellar orbits was decided from the frequency analysis.

5. Conclusions

From a methodological point of view, we see that the results of frequency analysis are in generally good agreement with those from the Liapunov exponents. The advantages of frequency analysis over Liapunov exponents are that the former needs much less computing time and, in addition to decide between regular and chaotic motion, it also allows the classification of the regular orbits.

Stellar orbits within globular clusters are highly chaotic. For the stars that (barely) reach the tidal limiting surface, the fraction of chaotic orbits may lie somewhere in between 50% and 90%. Nevertheless, it is even more surprising that the innermost parts of the cluster are also affected, and that as much as about 30% of the orbits that reach the half mass limiting surface might be chaotic.

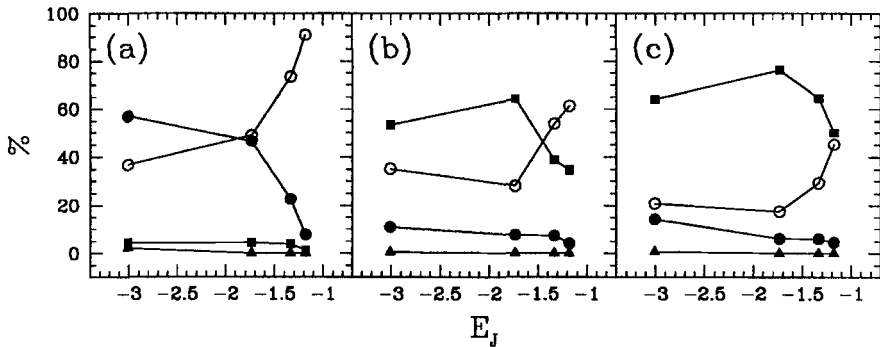Moreover, the Liapunov times we obtained for $E_J = -1.335$ are surprisingly

Fig. 6. Fractions of the different kinds of stellar orbits, for (a) the zero initial velocity, (b) $x–y$ and (c) $x–z$ plus $y–z$ start spaces. Filled circles: box orbits; filled triangles: long–axis tubes; filled squares: short–axis tubes; open circles: chaotic orbits.

short: they tend to crowd near 10 to 30 time units, while orbital periods are in the range between 1.4 and 7.5 time units. Not only is this short in terms of orbital periods but also in terms of cluster age: for the reasonable choice of units mentioned above, the cluster age would be about 50 to 100 time units, that is, longer than the Liapunov times. Evolution should thus be very fast, at least in the outermost parts of the cluster.

Long–axis tube orbits are very rare, even at the innermost parts of the cluster, while short–axis tubes are the most common orbits for non–zero initial velocity conditions. Box orbits only seem to dominate in the innermost parts, for zero velocity initial conditions. The scarcity of box orbits in the outermost, and most elongated, parts of the cluster may pose some problems to build self–consistent models. Such models should probably rely on the more abundant chaotic orbits but that might, in turn, complicate the building of stationary models, particularly considering the short Liapunov times detected here.

Acknowledgements

References

Binney, J. and Spergel D.: 1982, *ApJ*, **252**, 308
Binney, J. and Spergel D.: 1984, *MNRAS*, **206**, 159
Binney, J. and Tremaine, S.: 1987, *Galactic Dynamics*, Princeton University Press

Carpintero, D.D. and Aguilar, L.A.: 1998, *MNRAS,***298**, 1
Han, C. and Ryden, B.S.: 1994, *ApJ,***433**, 80
Laskar, J.: 1993,*Physica D,***67**, 257
Merritt, D. and Fridman T.: 1996, *ApJ,***460**, 136
Satoh, C.: 1980, *PASJ*, **32**, 41
Schwarzschild, M.: 1993, *ApJ*, **409**, 563